X-ray free electron laser studies of electron and phonon dynamics of graphene adsorbed on copper

Hirohito Ogasawara,[1] Han Wang,[1,7] Jörgen Gladh,[1,2] Alessandro Gallo,[1] Ralph Page,[1,2] Johannes Voss,[1] Alan Luntz,[1,*] Elias Diesen,[1] Frank Abild-Pedersen,[1] Anders Nilsson,[1,3] Markus Soldemo,[1,2,3] Marc Zajac,[2,8] Andrew Attar,[1] Michelle E. Chen,[2] Sang Wan Cho,[4] Abhishek Katoch,[4] Ki-Jeong Kim,[5] Kyung Hwan Kim,[6] Minseok Kim,[5] Soonnam Kwon,[5] Sang Han Park,[5] Henrique Ribeiro,[1,2] Sami Sainio,[1] Hsin-Yi Wang,[3] Cheolhee Yang,[6] and Tony Heinz[1,2]

[1]*SLAC National Accelerator Laboratory, 2575 Sand Hill Rd., Menlo Park, California 94025, USA*

[2]*Department of Applied Physics, Stanford University, Stanford, California 94305, USA*

[3]*Department of Physics, Stockholm University, Stockholm SE-10691, Sweden*

[4]*Department of Physics, Yonsei University, Wonju 26493, Korea*

[5]*Pohang Accelerator Laboratory, Pohang 37673, Korea*

[6]*Department of Chemistry, Pohang University of Science and Technology (POSTECH), Pohang 37673, Korea*

[7]*School of Physical Science and Technology, ShanghaiTech University, Shanghai 201210, China*

[8]*X-Ray Science Division, Argonne National Laboratory, Lemont, Illinois 60439, USA*

(Received 21 November 2022; accepted 26 January 2023; published 27 February 2023)

We report optical pumping and x-ray absorption spectroscopy experiments at the Pohang Accelerator Laboratory free electron laser that probes the electron dynamics of a graphene monolayer adsorbed on copper in the femtosecond regime. By analyzing the results with *ab initio* theory we infer that the excitation of graphene is dominated by indirect excitation from hot electron-hole pairs created in the copper by the optical laser pulse. However, once the excitation is created in graphene, its decay follows a similar path as in many previous studies of graphene adsorbed on semiconductors, i.e., rapid excitation of strongly coupled optical phonons and eventual thermalization. It is likely that the lifetime of the hot electron-hole pairs in copper governs the lifetime of the electronic excitation of the graphene.

DOI: 10.1103/PhysRevMaterials.7.024005

I. INTRODUCTION

Fundamental dynamical processes of adsorbates on metal surfaces following laser excitation are often in the femtosecond (fs) regime and this has spawned the field of femtochemistry at surfaces [1]. These have historically involved fs-laser optical pump–optical probe studies, with different optical nonlinear responses used to infer the dynamics, e.g., two-photon correlations, sum-frequency generation, etc. While these studies can be quite sensitive to the nuclear dynamics, they are rather insensitive to the actual electron dynamics. In contrast, photoemission and other x-ray spectroscopies probe the electronic structure of the adsorbate-substrate system and by combining them with optical pump techniques they can probe the dynamics of the electron states of the system. Optical pump–valence-band photoemission experiments can measure with high time, energy, and momentum resolution the temporal behavior of occupied valence bands of adsorbates or monolayer films on semiconductors. However, for adsorbates/films on metals both the metal and adsorbate/film contribute to the photoemission so that there can be ambiguity in the interpretation of the photoemission. X-ray spectroscopies such as x-ray absorption spectroscopy (XAS) and x-ray emission spectroscopies can also probe the electronic structure of the valence bands via the core to valence-band transition but in an element-specific and symmetry-selective way that completely isolates the electronic structure of the adsorbate/monolayer film from the metal. By combining such measurements with well-established theory one can also indirectly infer the adsorbate nuclear structure [2]. The emergence of x-ray free electron lasers (XFELs) over the past decade has opened up the possibility for optical pump–x-ray spectroscopy probe to more generally infer the electron dynamics of the adsorbate and by combining with theory to infer its nuclear dynamics, both occurring in the fs regime [3,4]. For example, studies of the CO oxidation on Ru(0001) have allowed observation of a species highly excited close to the transition state appearing $\sim$1 ps after initial optical excitation [5]. Similar experiments also allowed the observation of short-lived chemical transients in catalytic reactions that live for only $\sim$1.5 ps [6].

One phenomenon that is generally too fast for even the current generation of fs lasers or XFELs is to directly measure the lifetime of valence excited states of strongly bonded adsorbates on metal surfaces. This is because charge transfer between the adsorbate and metal surface is extremely fast, typically in the 1−3-fs time regime for strongly chemisorbed adsorbates and 10s of fs or longer for physisorbed species, and this limits the excited-state lifetimes to the same timescale [7]. However, the dynamic consequences of valence excitation can sometimes still be observed, especially

*acluntz@stanford.edu

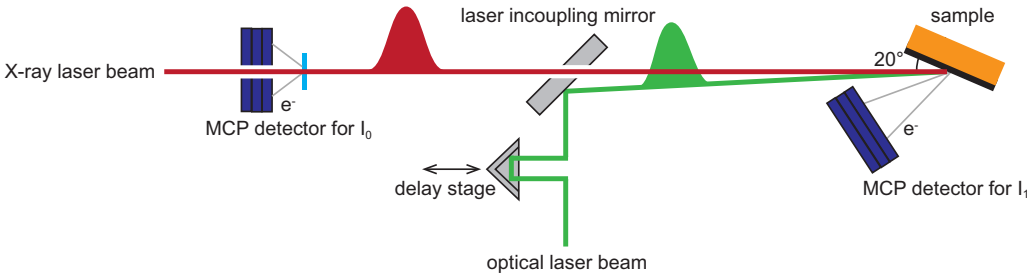

FIG. 1. Schematic of the experimental optical-pump–x-ray-spectroscopy probe for measuring femtosecond electron dynamics of graphene adsorbed on copper. The SSS beamline equips a collinear in-coupling geometry of the optical laser and x-ray beams, which maximize time resolution and ease of spatial alignment. An MCP (microchannel plate) detector for I_0 and I_1, respectively, monitors the intensity of incoming x-ray beam and absorbed x ray by the sample.

for physisorbed species with somewhat longer excited-state lifetimes. Graphene adsorbed on copper is a well-known example of weak adsorbate bonding and has been well studied structurally since chemical vapor deposition (CVD) growth of graphene on copper is a commercial process for producing graphene. Because of the importance of graphene in emerging electronics and optoelectronics applications, there have been a large number of fs transient optical adsorption and photoemission studies of excited graphene's hot-carrier dynamics, usually when free-standing or supported on semiconductors such as SiC or insulator materials such as quartz [8–12]. These show that the initially created hot electron and hole pairs ($e-h$) in graphene at 1/2 $\hbar\omega_{\text{optical}}$ rapidly ($\sim$20 fs) form a hot quasithermal distribution of $e-h$ pairs through interband scattering followed by energy transfer to a few strongly coupled optical phonons (SCOPs) on timescales of $\sim$200 fs. The SCOPs act as a bottleneck for further $e-h$ cooling, which is then dominated by the energy transfer from the SCOPs to the remaining phonons of Gr occurs on $\sim$1−3-ps timescales, with the rate likely dependent on both defect concentrations (supercollisions) and optical pump fluence. The overall cooling of carriers following optical excitation is generally described by a three-temperature model (3T) with separate temperatures for the hot carriers, the SCOPs, and the acoustic phonon bath [12–15].

In this paper, we report measurements of the valence electronic structure of a weakly adsorbed graphene overlayer on a metallic copper substrate (Gr/Cu) following fs optical laser excitation at 400 nm using the Pohang Accelerator Laboratory (PAL) free electron x-ray laser as probe [16,17]. We utilize C K-edge XAS to study the temporal evolution in the π- and π^* valence bands of graphene following the pulsed optical laser excitation and with theory infer some of the fs-resolved nuclear dynamics occurring after the optical pump.

II. METHODS

Figure 1 shows a diagram of the experiment. An optical pump (400 nm, 3.1-eV photon energy, pulse width 100 fs) and x-ray probe (near the C 1s absorption edge, 281−290-eV photon energy, pulse width 50 fs) beams are incident collinearly on a flat Gr/Cu surface at a 20° grazing-incidence geometry. The relative timing between the pump and probe beams is controlled with an optical delay line, with the spatial and temporal overlap (delay = 0) set by fluorescence of a thin cerium-doped yttrium aluminum garnet crystal. We estimate a temporal resolution of $\sim$150 fs in the delay from the temporal fits to the spectral changes, and is largely limited by optical and x-ray beam spatial fluctuations. We record the C 1s XAS by Auger electron yield using a biased partial electron-yield detector. The optical laser was p polarized to induce strong optical adsorption in the Cu. The x-ray probe beam was also p polarized, in which XAS dominantly sees the excitations involving π- or π^* valence bands of Gr/Cu in the grazing-incidence geometry. Transient response in the C 1s XAS after the optical pump can arise due to either occupation changes of π- and π^* valence bands or structural modifications of the Gr. All experimental details are given in the Supplemental Material [18] (see also Refs. [16,17,19] therein).

III. RESULTS AND DISCUSSION

Figure 2(a) (top) shows the XAS of Gr/Cu in the region of the π^* resonance. The spectra are dominated by the excitation from a C 1s to the π^* valence band of Gr. We also recorded high-resolution C 1s x-ray photoemission spectroscopy (XPS) of the Gr/Cu sample at a synchrotron beamline (Stanford Synchrotron Radiation Lightsource at SLAC). The Fermi level in the XAS spectrum is at 284.4 eV as obtained from the peak of the C 1s XPS spectrum [20]. This XAS spectrum is nearly identical to that of graphite, which has been much discussed in the literature [21–24]. The central π^* peak is thought to be highly excitonic in nature with the electron excited to the Gr valence band localized on the same C with the 1s hole. The region at energies higher than the central peak is thought to arise when the excited electron in the π^* valence band is not excitonic and therefore not localized on the C with the 1s hole [21]. There are also higher-energy σ^* resonances that could not be accessed due to the limited energy range in the PAL experiment.

The changes in the XAS spectrum induced by the optical laser (ΔXAS) at several fixed delay times between the x-ray pulse and the optical laser pulse are shown in the lower part of Fig. 2(a). The spectra are obtained by repetitive laser-on–laser-off measurements at each x-ray energy. Longer temporal delays are given in Fig. S1 [18] for Gr/Cu, which shows that the XAS nearly fully recovers to its original spectra over some $\sim$1000 ps. A two-dimensional (2D) representation of ΔXAS from similar experiments but taken by scanning the delay at

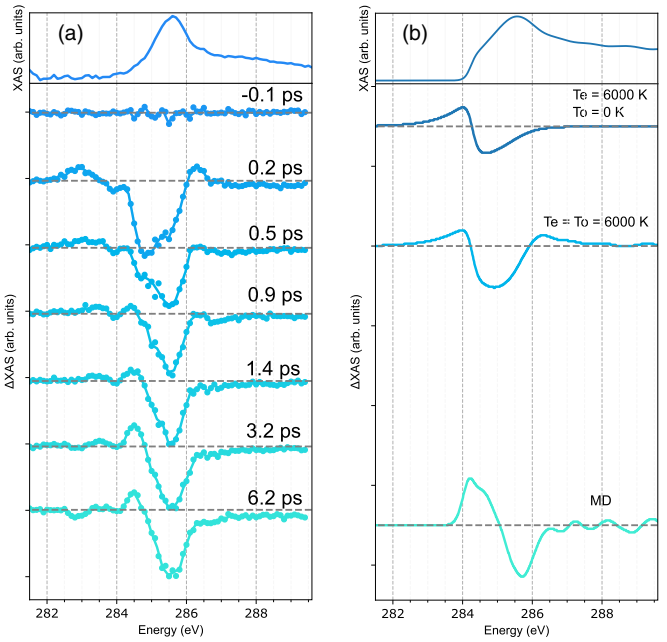

FIG. 2. (a) XAS spectra of Gr/Cu (top) and ΔXAS spectra of Gr/Cu for the labeled delay times between the optical pump and x-ray probe lasers. The negative delay probes the unexcited sample. (b) Theoretical XAS and ΔXAS of a Gr layer for the cases labeled that represent various stages of Gr temporal evolution; $T_e = 6000$ K represents the shortest delay times probed in the experiment) when only thermalized electronic excitation occurs, $T_e = T_o = 6000$ K represents the shortest delay times probed with both electronic and SCOPS excitation, and MD qualitatively represents the longest delay times probed.

modest time resolution and several fixed energies is given in Fig. 3.

The ΔXAS show several distinct short-lived changes plus some longer-lasting ones. There are transient increases in ΔXAS at 282.8 and 286.4 eV, a transient decrease in ΔXAS at

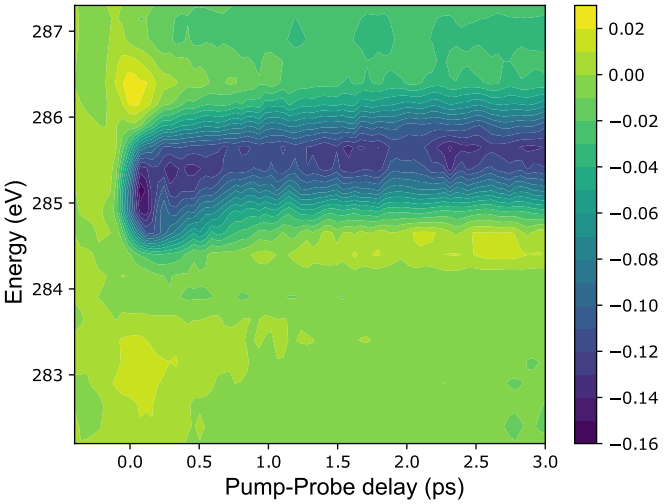

FIG. 3. Two-dimensional representation of ΔXAS of Gr/Cu in terms of x-ray energy and delay relative to the optical pulse. The heat map is given to the side.

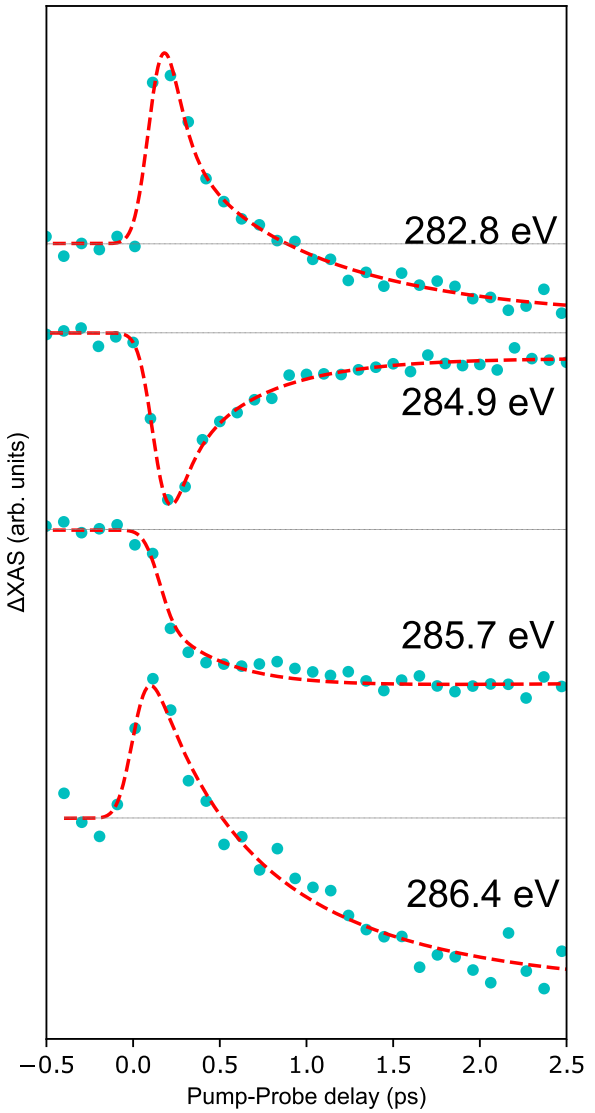

FIG. 4. Temporal response of ΔXAS of Gr/Cu at the principal features where changes occur in the ΔXAS. The intensity of each scan was normalized by the absolute value at the peak maximum. Curves represent biexponential or single-exponential fits to the data plus a step background change in Cu photoelectrons caused by the optical laser.

284.9 eV, and a long-lived decrease in ΔXAS at 285.7 eV near the XAS peak. The temporal responses of the principal features of the ΔXAS were obtained by high temporal-resolution scans at the fixed energies at or near these features and are shown in Fig. 4.

In all cases the rise times of the features is likely determined by temporal resolution of the experiments, ∼150 fs. However, the decay times observed are certainly longer than the experimental temporal resolution. In these plots, we account for changes in the XAS background (x-ray-induced nonresonant electron emission from the copper substrate) caused by the optical laser, as a step down following the optical laser and with a 100-ps recovery time. Although the decays are likely quite complex, we fit double exponentials as ∼85 fs and 1 ps at 282.8 eV; 100 fs and 0.5 ps at 284.9 eV; and a single exponential of 350 fs at 285.7 and 1.1

ps at 286.4 eV. However, since the energies of these features may overlap several physical processes described below (plus the XAS background changes from the optical laser), we only consider the temporal results qualitatively.

Our qualitative interpretation of these results is that the transient increase in ΔXAS intensity at 282.8 eV is created by the holes produced by optical excitation in the formerly fully occupied Gr π band which then allows a C $1s \rightarrow \pi$ transition. This is equivalent to a partial release of the Pauli blocking in the C $1s \rightarrow \pi$ transition from the optical excitation. The transient decrease in ΔXAS intensity at 284.9 eV results dominantly from the increased population in the π^* band created by the optical excitation which lowers the C $1s \rightarrow \pi^*$ intensity. Equivalently, this can be ascribed to an increase of Pauli blocking in the C $1s \rightarrow \pi^*$ transition caused by the optical excitation. The transient increase in ΔXAS at 286.4 eV can arise from two sources: transfer of the initial hot electrons to SCOPs modes and a many-body effect caused by the increased population of delocalized electrons in the π^* band. The longer temporal decrease in ΔXAS at 285.7 eV is caused by excitation of both the SCOPs and their subsequent relaxation into the acoustic modes of Gr. Below, we discuss in more detail the basis for these interpretations.

Our CVD-prepared Gr/Cu sample is anticipated to be negatively doped so that the Fermi level is ∼0.4 eV above the undoped neutrality point (intersection of the occupied and unoccupied Dirac cones) of Gr, although the details of the doping can vary with synthesis conditions in the CVD. For the conditions of our experiment (thermal annealing to 300° C in UHV), a small gap and *n*-type doping has been observed [25,26]. When the Gr/Cu sample is irradiated by the intense optical laser pulse used in the experiments (22-mJ/cm^2 absorbed optical fluence), the conventional two-temperature model (2T) for electrons and phonons in the copper substrate implies that the electrons are rapidly heated to $T_e \sim 10\,000$ K, followed by a relatively slow thermalization with the lattice modes over several ps to an equilibrium temperature of $T \sim 800$ K. The 2T model for the conditions of our experiments is shown in Fig. S3 [18] (see also Refs. [27,28] therein). The hot electrons and holes in the Cu can excite the Gr valence bands via charge-transfer processes. In addition, direct optical excitation of the Gr overlayer can also occur and is usually described in terms of the three-temperature model (3T) model. For the conditions of our experiments the 3T model also predicts high direct excitation of carriers in Gr, but the rapid excitation of the SCOPs limits the electron temperature rise in our observable time regime to ∼6000 K (estimated absorbed optical fluence 0.6 mJ/cm^2); see Fig. S4 [18] (see also Ref. [13] therein).

The incident optical laser fluence dependence was studied over the range 12−32 mJ/cm^2, corresponding to 4000−10 000 K peak electronic temperatures in the Gr/Cu. This range is limited by signal/noise issues on the low end and by optical damage of the Gr/Cu on the high end, but is always in a very high electronic temperature regime. No changes in the temporal response of the transient ΔXAS feature at 284.9 eV due to increased electron population in the π^* band were observed, only nearly linear changes in intensity. We anticipate that the time for initial thermalization of the electronic temperature in Gr/Cu would be fluence dependent, but these times are shorter than the time resolution of our experiments (150 fs) so were not observable.

Because most of the optical energy is deposited into the Cu substrate, we believe that the dominant electronic excitation of Gr occurs from indirect charge-transfer processes from the hot electrons and holes created in the Cu substrate. Evidence for this is that the holes created in the Gr π-band peak ∼1.7 eV below the Fermi level in the ΔXAS and hot electrons peak ∼0.5 eV above the Fermi level in the ΔXAS. If direct optical excitation of Gr was dominate, then the holes created in the π band and the electrons excited in the π^* band should follow Fermi-Dirac distributions weighted by the density of the band states, i.e., both hot holes and electrons peaking close to the Fermi level in the ΔXAS, and this is what is observed for direct optical pumping of graphite [14] and *ab initio* theoretical simulations of ΔXAS for a pure Gr film at $T_e = 6000$ K as shown in Fig. 2(b). The *ab initio* calculations for XAS and ΔXAS of a Gr film are described in the Supplemental Material [18] (see also Refs. [2,29–35] therein). On the other hand, at 10 000 K and even 6000 K the hot holes in Cu are dominated by the *d* band, even though it is ∼2 eV below the Fermi energy (E_F), while hot electrons peak in the *sp* band near E_F. This is shown in Fig. S5. However, because injection of holes (electrons) from Cu into Gr occurs through the dipole field created by the *n*-type doping of Gr, the holes created in Gr will be created at a slightly lower energy than 2 eV relative to E_F. In a similar manner, the hot electrons in Gr will be created at slightly higher energies relative to E_F. Both shifts are consistent with the hot-hole and hot-electron peaks observed in the ΔXAS as arising from that of Cu. This suggests that the electronic coupling between Gr and Cu is so strong that after initial excitation both the Gr- and Cu excited states evolve together temporally and are limited by the excitation lifetime in the Cu. This is likely why excited valence states of Gr adsorbed on Cu can appear to exist for ∼300 fs despite a lower inherent lifetime.

While the excitation and decay of hot carriers in Gr/Cu qualitatively rationalizes the transient changes in the XAS observed at 282.8 and 284.9 eV [Fig. 2(b)], it does not explain the other changes observed in the XAS. The cooling of the hot carriers in free-standing or semiconductor-supported Gr and graphite via intraband scattering to the SCOPs and then subsequent decay of the SCOPs into the acoustic modes has been well studied. In order to understand if these same processes qualitatively rationalize the remaining spectral changes observed in XAS, we have made *ab initio* theoretical calculations of the XAS for a pure Gr layer that simulate both short-time and long-time behavior that also include excitation of the phonon modes in Gr. For the short-time behavior, we assume that rapid cooling of the hot carriers to 6000 K occurs and that we also populate the SCOPs ($A_1^{'} + E_{2g}$) modes near the Γ- and *K* points, respectively, in the Brillouin zone to 6000 K; see the 3T model in Fig S4 [18] (see also Ref. [13] therein). For the long-time behavior, we assume that the Gr cools to a thermal equilibrium and average the XAS for 50 snapshots of the instantaneous structure taken from an *ab initio* molecular dynamics simulation. Details of both calculations are given in the Supplemental Material. The results of both calculations are also shown in Fig. 2(b), which compare to the experimental results for 0.2 and

6.2 ps, respectively. In addition to the transient changes due to hot-carrier excitations, we see that excitation of the SCOPS also causes a decrease in the ΔXAS peak height at 285.7 eV as well as an increase in ΔXAS at 286.4 eV caused by a slight blueshift of the peak. Both agree qualitatively with the transient changes in ΔXAS observed in the experiments at 0.2−0.5 ps. The calculated ΔXAS via molecular dynamics qualitatively shows that the decrease in the peak intensity and an increase below the peak at ∼ 284.7 eV (due to a slight redshift in the peak) observed at 3.2 and 6.2 ps are qualitatively consistent with a longer-time thermal distribution of the Gr. Similar changes have been predicted theoretically in other calculations of temperature-dependent spectra of graphene [8–12,22] and are confirmed by static measurements of the temperature dependence in ΔXAS of our samples via synchrotron XAS measurements (see Fig. S2 [18]).

The excitation of SCOPs may not be the only possible mechanism responsible for the feature in the ΔXAS at 286.4 eV. Since this feature is entirely absent in density-functional theory (DFT) calculations of hot-carrier excitation [see Fig. 2(b)], we suggest that this could also arise from a many-body effect not included in DFT. The excitation of valence π^* electrons in Gr indirectly from hot carriers in Cu should create a delocalized excitation in Gr and is not anticipated to affect the intensity of the localized excitonic resonance predominately, but rather the higher nonexcitonic XAS energy regime. A similar transient increase in intensity in the high-energy side of the XAS peak at ∼286.4 eV was also observed in optically pumped graphite [14]. We suspect that the same two mechanisms suggested for Gr/Cu could also be responsible for this feature in graphite as well since optical pumping will also create SCOPs and excitations in the delocalized valence band.

Although a theoretical study of the fully coupled electron dynamics of Gr/Cu is beyond the scope of this paper, comparison of the 2T and 3T models in Figs. S3 and S4 [18] (see also Refs. [13,27,28] therein) which are based on uncoupled components suggest that in the short observable timescales (<500 fs), that T_e of Cu > T_e of Gr, and that this defines the principal direction of electronic excitation as discussed above. After the indirect electronic excitation of Gr, rapid coupling to the SCOPS occurs, followed by a slower decay of the SCOPs into the acoustic modes of Gr. This aspect is quite similar to the many optical-pumping studies of Gr on semiconductors and insulators [8–11] and could account for the observed bi-exponential dependence of the hot-hole and electron features at 282.8 and 284.9 eV, respectively. However, for Gr/Cu the strong electronic coupling of Gr to Cu we believe means that the T_e of Gr and Cu evolve together so that the time dependence of the hot hole and hot electrons in Gr reflect the nonexponential lifetimes of the electronic excitations in Cu. We anticipate that there is little direct coupling of the phonons of Gr with phonon modes in Cu in these short-time regimes because of the large interplanar distance of Gr to Cu of ∼3.3 Å [26]. However, over periods of ∼1000 ps it appears that the Gr thermalizes with the Cu and the entire Gr/Cu cools to its ambient since the XAS recovers to that prior to the optical laser (see Fig. S1 [18]). This long recovery time of the XAS is related to the slow thermal cooling of the entire Gr/Cu film to its support and does not reflect the Gr-to-Cu cooling time which is presumably much shorter. Time-domain transient reflectance experiments on Gr/Cu have been interpreted to suggest strong phonon coupling between Gr and Cu in the ps regime, but they neglect charge transfer and its effects on the reflectivity in the short-time regime [36].

IV. CONCLUSIONS

In this paper we have shown that fs optical pumping and x-ray absorption spectroscopy at the PAL free electron laser can probe the electron dynamics of a graphene monolayer adsorbed on Cu in the femtosecond regime. By analyzing the results with *ab initio* theory we infer that the excitation of graphene is dominated by indirect excitation from hot electron-hole pairs created in the Cu by the optical pulses. However, once the excitation is created in graphene, its decay follows a similar path as in many previous studies of graphene adsorbed on semiconductors, i.e., rapid excitation of SCOPS and eventual thermalization. It is likely that the lifetime of Cu hot electron-hole pairs governs the lifetime of the electronic excitation of the adsorbed graphene.

While Gr electron and phonon dynamics have previously been studied extensively by other pump-probe experiments, e.g., optical-pump–valence-band photoemission, these studies are generally only possible when the Gr is free-standing or supported on semiconductors. We show here that pump-probe experiments using XAS at an XFEL as probe allows one to study electron and phonon dynamics of adsorbates/films on metallic substrates as well. As an example, we find that the optical excitation mechanism is different with Gr adsorbed on metals than on semiconductors, but that the decay of Gr excitations was similar and in good semiquantitative agreement with the prior measurements of Gr dynamics on semiconductors.

ACKNOWLEDGMENTS

This research was supported by the U.S. Department of Energy, Office of Science, Office of Basic Energy Sciences, Chemical Sciences, Geosciences, and Biosciences Division, Catalysis Science Program to the Ultrafast Catalysis FWP 100435 at SLAC National Accelerator Laboratory under Contract No. DE-AC02-76SF00515. This study was also partly supported by the National Research Foundation of Korea (Grant No. NRF-2020R1A2C1007416). We gratefully acknowledge the technical support by the XFEL accelerator and beamline divisions at Pohang Accelerator Laboratory (PAL-XFEL), and the Stanford Synchrotron Radiation Lightsource (SSRL), SLAC National Accelerator Laboratory. The experiments at SSS endstation of PAL-XFEL (Proposals No. 2020-first-SSS-006 and No. 2020-second-SSS-014) funded by the Ministry of Science and ICT, South Korea. Use of SSRL is supported by the U.S. Department of Energy, Office of Science, Office of Basic Energy Sciences under Contract No. DE-AC02-76SF00515.

[1] C. Frischkorn and M. Wolf, Femtochemistry at metal surfaces: Nonadiabatic reaction dynamics, Chem. Rev. **106**, 4207 (2006).

[2] E. Diesen, G. L. S. Rodrigues, A. C. Luntz, F. Abild-Pedersen, L. G. M. Pettersson, and J. Voss, Accuracy of XAS theory for unraveling structural changes of adsorbates: CO on Ni(100), AIP Adv. **10**, 115014 (2020).

[3] E. Diesen, H.-Y. Wang, S. Schreck, M. Weston, H. Ogasawara, J. LaRue, F. Perakis, M. Dell'Angela, F. Capotondi, L. Giannessi, E. Pedersoli, D. Naumenko, I. Nikolov, L. Raimondi, C. Spezzani, M. Beye, F. Cavalca, B. Liu, J. Gladh, S. Koroidov, P. S. Miedema, R. Costantini, T. F. Heinz, F. Abild-Pedersen, J. Voss, A. C. Luntz, and A. Nilsson, Ultrafast Adsorbate Excitation Probed with Subpicosecond-Resolution X-Ray Absorption Spectroscopy, Phys. Rev. Lett. **127**, 016802 (2021).

[4] H.-Y. Wang, S. Schreck, M. Weston, C. Liu, H. Ogasawara, J. LaRue, F. Perakis, M. Dell'Angela, F. Capotondi, L. Giannessi, E. Pedersoli, D. Naumenko, I. Nikolov, L. Raimondi, C. Spezzani, M. Beye, F. Cavalca, B. Liu, J. Gladh, S. Koroidov, P. S. Miedema, R. Costantini, L. G. M. Pettersson, and A. Nilsson, Time-resolved observation of transient precursor state of CO on Ru(0001) using carbon K-edge spectroscopy, Phys. Chem. Chem. Phys. **22**, 2677 (2020).

[5] H. Öström, H. Öberg, H. Xin, J. LaRue, M. Beye, M. Dell'Angela, J. Gladh, M. L. Ng, J. A. Sellberg, S. Kaya, G. Mercurio, D. Nordlund, M. Hantschmann, F. Hieke, D. Kühn, W. F. Schlotter, G. L. Dakovski, J. J. Turner, M. P. Minitti, A. Mitra, S. P. Moeller, A. Föhlisch, M. Wolf, W. Wurth, M. Persson, J. K. Nørskov, F. Abild-Pedersen, H. Ogasawara, L. G. M. Pettersson, and A. Nilsson, Probing the transition state region in catalytic CO oxidation on Ru, Science **347**, 978 (2015).

[6] J. LaRue, O. Krejčí, L. Yu, M. Beye, M. L. Ng, H. Öberg, H. Xin, G. Mercurio, S. Moeller, J. J. Turner, D. Nordlund, R. Coffee, M. P. Minitti, W. Wurth, L. G. M. Pettersson, H. Öström, A. Nilsson, F. Abild-Pedersen, and H. Ogasawara, Real-time elucidation of catalytic pathways in CO hydrogenation on Ru, J. Phys. Chem. Lett. **8**, 3820 (2017).

[7] G. Dutton, D. P. Quinn, C. D. Lindstrom, and X.-Y. Zhu, Exciton dynamics at molecule-metal interfaces: C_{60} / Au (111), Phys. Rev. B **72**, 045441 (2005).

[8] M. Massicotte, G. Soavi, A. Principi, and K.-J. Tielrooij, Hot carriers in graphene – fundamentals and applications, Nanoscale **13**, 8376 (2021).

[9] I. Gierz, J. C. Petersen, M. Mitrano, C. Cacho, I. C. E. Turcu, E. Springate, A. Stöhr, A. Köhler, U. Starke, and A. Cavalleri, Snapshots of non-equilibrium Dirac carrier distributions in graphene, Nat. Mater. **12**, 1119 (2013).

[10] J. C. Johannsen, S. Ulstrup, F. Cilento, A. Crepaldi, M. Zacchigna, C. Cacho, I. C. E. Turcu, E. Springate, F. Fromm, C. Raidel, T. Seyller, F. Parmigiani, M. Grioni, and P. Hofmann, Direct View of Hot Carrier Dynamics in Graphene, Phys. Rev. Lett. **111**, 027403 (2013).

[11] D. Brida, A. Tomadin, C. Manzoni, Y. J. Kim, A. Lombardo, S. Milana, R. R. Nair, K. S. Novoselov, A. C. Ferrari, G. Cerullo, and M. Polini, Ultrafast collinear scattering and carrier multiplication in graphene, Nat. Commun. **4**, 1987 (2013).

[12] J. C. W. Song and L. S. Levitov, Energy flows in graphene: Hot carrier dynamics and cooling, J. Phys.: Condens. Matter **27**, 164201 (2015).

[13] C. H. Lui, K. F. Mak, J. Shan, and T. F. Heinz, Ultrafast Photoluminescence from Graphene, Phys. Rev. Lett. **105**, 127404 (2010).

[14] T. P. H. Sidiropoulos, N. Di Palo, D. E. Rivas, S. Severino, M. Reduzzi, B. Nandy, B. Bauerhenne, S. Krylow, T. Vasileiadis, T. Danz, P. Elliott, S. Sharma, K. Dewhurst, C. Ropers, Y. Joly, M. E. Garcia, M. Wolf, R. Ernstorfer, and J. Biegert, Probing the Energy Conversion Pathways between Light, Carriers, and Lattice in Real Time with Attosecond Core-Level Spectroscopy, Phys. Rev. X **11**, 041060 (2021).

[15] H. Wang, J. H. Strait, P. A. George, S. Shivaraman, V. B. Shields, M. Chandrashekhar, J. Hwang, F. Rana, M. G. Spencer, C. S. Ruiz-Vargas, and J. Park, Ultrafast relaxation dynamics of hot optical phonons in graphene, Appl. Phys. Lett. **96**, 081917 (2010).

[16] S. H. Park, J. Yoon, C. Kim, C. Hwang, D.-H. Kim, S.-H. Lee, and S. Kwon, Scientific instruments for soft x-ray photon-in/photon-out spectroscopy on the PAL-XFEL, J. Synchrotron Radiat. **26**, 1031 (2019).

[17] S. H. Park, M. Kim, C.-K. Min, I. Eom, I. Nam, H.-S. Lee, H.-S. Kang, H.-D. Kim, H. Y. Jang, S. Kim, S. Hwang, G.-S. Park, J. Park, T.-Y. Koo, and S. Kwon, PAL-XFEL soft x-ray scientific instruments and x-ray optics: First commissioning results, Rev. Sci. Instrum. **89**, 055105 (2018).

[18] See Supplemental Material at http://link.aps.org/supplemental/10.1103/PhysRevMaterials.7.024005 for additional experimental and theoretical results.

[19] R. McLaren, S. A. C. Clark, I. Ishii, and A. P. Hitchcock, Absolute oscillator strengths from k -shell electron-energy-loss spectra of the fluoroethenes and 1,3-Perfluorobutadiene, Phys. Rev. A **36**, 1683 (1987).

[20] A. Nilsson, O. Björneholm, E. O. F. Zdansky, H. Tillborg, N. Mårtensson, J. N. Andersen, and R. Nyholm, Photoabsorption and the unoccupied partial density of states of chemisorbed molecules, Chem. Phys. Lett. **197**, 12 (1992).

[21] P. A. Brühwiler, A. J. Maxwell, C. Puglia, A. Nilsson, S. Andersson, and N. Mårtensson, π^* and Σ^* Excitons in C 1s Absorption of Graphite, Phys. Rev. Lett. **74**, 614 (1995).

[22] W. Olovsson, T. Mizoguchi, M. Magnuson, S. Kontur, O. Hellman, I. Tanaka, and C. Draxl, Vibrational effects in x-ray absorption spectra of two-dimensional layered materials, J. Phys. Chem. C **123**, 9688 (2019).

[23] O. Wessely, O. Eriksson, and M. I. Katsnelson, dynamical core-hole screening in the x-ray absorption spectra of graphite, C 60, and carbon nanotubes: A first-principles electronic structure study, Phys. Rev. B **73**, 075402 (2006).

[24] R. E. Ovcharenko, I. I. Tupitsyn, E. P. Savinov, E. N. Voloshina, B. Paulus, Yu. S. Dedkov, and A. S. Shulakov, Specific many-electron effects in x-ray spectra of simple metals and graphene, Phys. Chem. Chem. Phys. **15**, 6749 (2013).

[25] A. J. Marsden, M. Asensio, J. Avila, P. Dudin, A. Barinov, P. Moras, P. M. Sheverdyaeva, T. W. White, I. Maskery, G. Costantini, N. R. Wilson, and G. R. Bell, Is graphene on copper doped? Phys. Status Solidi RRL – Rapid Res. Lett. **7**, 643 (2013).

[26] G. Giovannetti, P. A. Khomyakov, G. Brocks, V. M. Karpan, J. van den Brink, and P. J. Kelly, Doping Graphene with Metal Contacts, Phys. Rev. Lett. **101**, 026803 (2008).

[27] S. I. Anisimov, B. L. Kapellovich, and T. L. Perel'man, Electron emission from metal surfaces exposed to ultrashort laser pulses, J. Exp. Theor. Phys. **39**, 375 (1974).

[28] M. Bonn, D. N. Denzler, S. Funk, M. Wolf, S.-S. Wellershoff, and J. Hohlfeld, Ultrafast electron dynamics at metal surfaces: Competition between electron-phonon coupling and hot-electron transport, Phys. Rev. B **61**, 1101 (2000).

[29] G. Kresse and J. Furthmüller, Efficient iterative schemes for *ab initio* total-energy calculations using a plane-wave basis set, Phys. Rev. B **54**, 11169 (1996).

[30] G. Kresse and D. Joubert, From ultrasoft pseudopotentials to the projector augmented-wave method, Phys. Rev. B **59**, 1758 (1999).

[31] J. P. Perdew, K. Burke, and M. Ernzerhof, Generalized Gradient Approximation Made Simple, Phys. Rev. Lett. **77**, 3865 (1996).

[32] M. Taillefumier, D. Cabaret, A.-M. Flank, and F. Mauri, X-ray absorption near-edge structure calculations with the pseudopotentials: Application to the K edge in diamond and α-quartz, Phys. Rev. B **66**, 195107 (2002).

[33] C. Gougoussis, M. Calandra, A. P. Seitsonen, and F. Mauri, First-principles calculations of x-ray absorption in a scheme based on ultrasoft pseudopotentials: From α-quartz to high- T c compounds, Phys. Rev. B **80**, 075102 (2009).

[34] P. Giannozzi, S. Baroni, N. Bonini, M. Calandra, R. Car, C. Cavazzoni, D. Ceresoli, G. L. Chiarotti, M. Cococcioni, I. Dabo, A. Dal Corso, S. de Gironcoli, S. Fabris, G. Fratesi, R. Gebauer, U. Gerstmann, C. Gougoussis, A. Kokalj, M. Lazzeri, L. Martin-Samos, N. Marzari, F. Mauri, R. Mazzarello, S. Paolini, A. Pasquarello, L. Paulatto, C. Sbraccia, S. Scandolo, G. Sclauzero, A. P. Seitsonen, A. Smogunov, P. Umari, and R. M. Wentzcovitch, QUANTUM ESPRESSO: A modular and open-source software project for quantum simulations of materials, J. Phys.: Condens. Matter **21**, 395502 (2009).

[35] L. Triguero, L. G. M. Pettersson, and H. Ågren, Calculations of near-edge x-ray-absorption spectra of gas-phase and chemisorbed molecules by means of density-functional and transition-potential theory, Phys. Rev. B **58**, 8097 (1998).

[36] Y. Lu, X. Tan, Y. Du, D. Ma, and W. Ma, Direct observation of ultrafast carrier coupling dynamics in monolayer graphene/metal system, Int. J. Heat Mass Transfer **197**, 123322 (2022).